INTERNATIONAL ATOMIC ENERGY AGENCY
UNITED NATIONS EDUCATIONAL, SCIENTIFIC AND CULTURAL ORGANIZATION
INTERNATIONAL CENTRE FOR THEORETICAL PHYSICS
I.C.T.P., P.O. BOX 586, 34100 TRIESTE, ITALY. CABLE CENTRATOM TRIESTE

H4-SMR 393/21

SPRING COLLEGE ON PLASMA PHYSICS

15 May - 9 June 1989

LASER PLASMA INTERACTION

J.L. Bobin

Laboratoire de Physique Nucleare et de Hautes Energies
Universite de Paris VI (Pierre et Marie Curie)
Tour 32 - Rdc
4. Place Jussieu
Paris F-75252 CEDEX 05
France

I.C.T.P. Trieste
Spring College in Plasma Physics 1989.

LASER PLASMA INTERACTION

J.L. BOBIN

Université Pierre et Marie Curie,

PARIS.

Table of contents.

1. Introduction.

High amplitude electron plasma waves with phase velocity close to c propagate large longitudinal electric fields which might be able to accelerate electrons up to energies of interest to elementary particle physics. Two methods have been proposed in order to generate such waves: resonant beating of two electromagnetic waves, wakes. Since in general high frequencies improve the performances in accelerator technology, many ideas stem from an extensive use of lasers (i.e. high fields at optical frequencies).

Pioneering theoretical investigations about laser beatwaves were done long ago, first by Montgomery [1] who set up the relevant system of 3 coupled rate equations, then by Rosenbluth and Liu [2] who, through a different approach, calculated the growth and saturation by relativistic detuning. Later, using particle in cell simulations, Tajima and Dawson [3] obtained computational evidence of electron acceleration. Then, extensive theoretical and numerical investigations were made together with a few experimental attempts. Limiting mechanisms were identified and evaluated. Rapidly, the strong connection with stimulated Raman scattering and with processes occuring in the free electron lasers became apparent. More recently it was realized that short high intensity pulses of laser light are also able to generate a wakefield whose main properties were calculated by Gorbunov and Kisanov [4].

The plasma in which the required electron waves are to be generated has to be reasonably long and should have a uniform electron density. Lasers can be also used to create such plasmas with prescribed size and electron density and temperature. The present review will deal first with this topic. A second part is to be devoted to wave generation. Finally the requirements on the lasers themselves will be examined.

Part I

LASER GENERATION OF PLASMAS

2. Overview.

The use of lasers is suited to plasma creation with electron densities in the range 10^{15}-10^{17} cm^{-3} through gas breakdown or the irradiation of solid surfaces or foils. In most of the cases, a high intensity is needed. The laser beam has to be focused. Thus the optical properties of the laser beam and of the focusing devices are of importance. They are summarized by 2 quantities: the diffraction limited spotsize σ (proportional to the focal length) and the Rayleigh length

$$L_R = \frac{\pi\sigma^2}{\lambda} \qquad (2-1)$$

where λ is the light wavelength. Inside the volume $\pi\sigma^2 L_R/2$, the laser intensity is fairly uniform. The values of σ and L_R are important to determine the requirements on laser power and energy.

Various methods were proposed to create plasmas suited to electron acceleration. Table 1 states the advantages and drawbacks of those which are to be reviewed in sections 3 to 5.

3. Multiphoton gas breakdown.

In ordinary gas breakdown, a high laser intensity at the focus of a lens or a mirror, releases first a few electrons by multiphotonic ionization. Through

inverse bremsstrahlung in presence of neutrals, these electrons gain enough energy to ionize further atoms. An exponential increase of the number of free electrons takes place (electron avalanche) until a high temperature plasma is created and set into laser driven motion: the so called optical detonation (for a review see e.g. Raizer [6] and references therein). In order for the breakdown to take place, the laser intensity should be larger than 10^{10} Wcm^{-2} at optical frequencies. The resulting plasma is far from homogeneous.

Complete multiphotonic ionization without subsequent motion is possible with high intensity short (picosecond) laser pulses, thus providing a satisfactorily homogeneous plasma, The number N of photons with energy $h\omega$ required to ionize the atom (ioniation potential χ_i) is

$$N = 1 + \mathrm{Int}\left(\frac{\chi_i}{h\omega}\right) \qquad (3-1)\,.$$

It is then a priori expected that the probability for ionization with a laser intensity I goes as I^N. Experiments show such a dependance, often with an exponent slightly smaller than N.

Now, the degree of ionization is a very rapidly increasing function of the intensity. As shown on figure 3-1, multiphoton ionization is effective only at high intensities. The laser beam has to be focused and the fully ionized plasma is created over a distance equal to twice the Rayleigh length. The plasma electron density is of course as uniform as the initial gas.

Choose as an example hydrogen (χ_i =13.6 e.V.) and a Nd laser ($h\omega$ = 1.17 e.V.). Then N=12. However, fitting experiments, the exponent is about 10. Expressed in terms of electric field (in V/cm) the probability w of ionization is approximately:

$$w = 10^{-137}E^{20} \qquad (3\text{-}2).$$

For a picosecond laser pulse to completely ionize hydrogen with initial atomic density 10^{17} cm^{-3}, the necessary field turns out to be $2\,10^{8}$ V/cm i.e. an intensity 10^{14} Wcm^{-3}. This technique was succesfully used at the Rutherford lab in U.K.[5]. Unfortunately, as can be seen on the above example, the efficiency of direct complete multiphotonic ionization is rather poor, something like $6\,10^{-5}$.

4. Resonant gas breakdown.

In resonant breakown of a Na vapor, the tuned radiation saturates the 3S-3P transition. When the incoming intensity is large enough, 3/4 th of the atoms are in the 3P state which can be considered as a pseudo ground state for Boltzmann equilibrium. A few free electron are created by two photon ionization. Then multiplication proceeds via 2 possible channels:

i) initial free electrons undergo superelastic collisions with 3P states and are able to ionize after 3 such collisions.

ii) collisions between atoms in the 3P state produce either atoms excited to higher states (energy pooling). Subsequent collisions lead to Penning ionization:

energy pooling: $Na(3P) + Na(3P) \rightarrow Na(3S) + Na(n)$

Penning ionization: $Na(3S) + Na(n) \rightarrow Na(3S) + Na^{+} + e$

with balance $3Na(3P) \rightarrow 2Na(3S) + Na^{+} + e.$

Alternatively, Sodium atoms in the 3P state are able to form a molecular ion

associative ionization: $Na(3P) + Na(3P) \rightarrow Na_2^{+} + e$

followed by dissociation: $Na_2^{+} \rightarrow Na(3S) + Na^{+}.$

Eventually, a motionless low temperature plasma is produced whose high degree of ionization lasts as long as the laser beam is on. The resonant breakdown is obtained at comparatively low laser intensities: typically 10^{6} Wcm^{-2}.

The time history of the particle density N_α of species α is given by a rate equation. The system of rate equations, completed by equations for the energy density W and the electron temperatur T_e, is solved computationally. The results are best represented on a triangular diagram for the densities N_S and N_P of atoms in the 3S and 3P state and the electron density N_e (figure 4-1). All trajectories with initial conditions N_S=N_a(the initial density of neutral atoms), T_e=0, pass in the vicinity of a saddle point S which represents the pumped vapor in saturated state, and end at a node N very close to N_e=N_a, i.e. an almost complete ionization. Meanwhile, T_e stays at very low values unconsistent with Saha's equation.

The computations evidence other interesting features. First, the time necessary to reach the highly ionized state varies as the reciprocal of the initial atomic density. Its value is about 30 ns at $N_a = 10^{17}$cm^{-3}. The eventual degree of ionization slightly diminishes as N_a increases (90% at 10^{18}cm^{-3}). The electron temperature, almost independant of N_a is well below 1 e.V. It decreases by 10% as the ionization reaches its maximum (figure 4-2a). The time history of the electron density is given on figure 4-2b. Finally, it is found that maximum values

of the populations in the excited states above 3P, are orders of magnitude below N_a.

In the experiments, a tunable laser beam is aimed at a saturated Sodium vapour elaborated in a heat pipe with Argon as a buffer. The time history of the electron temperature and density is inferred from time resolved spectroscopic measurements: occurence, shift and broadening of atomic lines. Results are shown on figure 4-3 for an initial atomic density slightly below 10^{17} cm^{-3} [7]. The gas is almost totally ionized during the laser pulse (FWHM 2μs). This is followed by a recombination stage in which exists a plateau regime: the degree of ionization and the plasma temperature remain constant for about 50μs. Since the required laser intensity is moderate, there is no need for strong focusing. Such plasmas may be obtained in long filaments. Since the obtained plasma has a very low electron temperature, most of the laser energy has been used for ionization, i.e. the efficiency is high.

The method cannot be applied to hydrogen. Indeed there is no available tunable laser source around the frequency of the 1s-2p transition (Lyman α: λ=121.6 nm, ω=1.55 $10^{16}s^{-1}$).

5. Exploding foils and surface ablation.

When a high iontensity laser beam impinges onto a solid surface, energy is absorbed by the material. A high temperature plasma is formed and is set into motion.

In the case of a thin foil, the whole foil explodes. The plasma expands in both directions perpendicular to the surface in a symetric fashion. The time varying plasma density has a maximum at the plane of symetry. The density profile can be monitored accurately by plasma interferometry. The region in which the density can be considered as uniform is restricted to the vicinity of the plane of symetry (figure 5-1).

At the surface of a thick material, a plasma plume is formed the shape of which can be controlled by a suitable laser irradiation. By focusing with a cylindrical length, or setting up a succession of aligned foci, each corresonding to a different beam, a long plasma filament parallel to the surface can be created. The density profile is well known. Regions exist in which the electron density is fairly uniform along a direction parallel to the surface (figure 5-2).

All the tricks which have been invented to build up long plasmas aimed at X-ray laser experiments, are also well suited for the generation of high amplitude electron waves which propagate (see e.g. [8]).

Part II

Laser driven plasma waves

6. Relativistic equations of motions.

Consider a particle with electric charge q moving under the influence of an electromagnetic field. The momentum energy 4-vector

$$(\mathbf{p},W) = (m_0\gamma\mathbf{v}, m_0\gamma c^2) \qquad (6\text{-}1)$$

and the 4-potential $(\mathbf{A},\emptyset)$, enters the usual equations of motion

$$\frac{d\mathbf{p}}{dt} = q\left(\mathbf{E}+\mathbf{v}\times\mathbf{B}\right) = q\left[-\nabla\emptyset - \frac{\partial\mathbf{A}}{\partial t} - (\mathbf{v}\cdot\nabla)\mathbf{A} + \nabla(\mathbf{v}\cdot\mathbf{A})\mathbf{A}\right]$$

$$\frac{dW}{dt} = q\left(\mathbf{E}+\mathbf{v}\times\mathbf{B}\right)\mathbf{v} = q\left(-\nabla\emptyset - \frac{\partial\mathbf{A}}{\partial t}\right)\mathbf{v}$$

Whenever in plane waves, the scalar potential $\emptyset$ has a purely longitudinal gradient and the vector potential A is purely transverse, one gets, after some algebra, the relevant equations:

$$\frac{dv_z}{dt} = -\frac{q}{m_0\gamma^3}\frac{\partial\emptyset}{\partial z} - \left(\frac{q}{\gamma m_0}\right)^2\frac{\partial|\mathbf{A}|^2}{\partial z} - \left(\frac{q}{\gamma m_0}\right)^2\left(\frac{v_z}{2c^2}\right)\frac{\partial|\mathbf{A}|^2}{\partial t}$$

$$\frac{d\gamma}{dt} = \left(\frac{q}{m_0c^2}\right)v_z\frac{\partial\emptyset}{\partial z} + \left(\frac{q^2}{2\gamma m_0^2c^2}\right)\frac{\partial|\mathbf{A}|^2}{\partial t}$$

They can be applied to individual electrons isolated or in bunches, and to the electron fluid in a plasma as well.

For the electron fluid in the field of 2 electromagnetic waves, a purely transverse field, $\emptyset$ is zero and the vector potential **A** is a relativistic invariant. Assume for convenience that **A** results from 2 circularly polarized waves in the laboratory frame:

$$\mathbf{A}_1 = [A_1\cos(k_1z-\omega_1t+\varphi_1),\ A_1\sin(k_1z-\omega_1t+\varphi_1),\ 0]$$

$$\omega_1 > \omega_2 \qquad (6\text{-}4).$$

$$\mathbf{A}_2 = [\pm A_2\cos(k_2z\mp\omega_2t+\varphi_2),\ A_2\sin(k_2z\mp\omega_2t+\varphi_2),\ 0]\ .$$

The upper sign means that both waves propagate in the same direction, the lower sign that they propagate in opposite directions. The vector potential enters the equations of motion through its modulus squared only:

$$|\mathbf{A}|^2 = A_1^2 + A_2^2 \pm 2A_1A_2\cos\left[(k_1\mp k_2)z-(\omega_1-\omega_2)t+\Delta\varphi\right] \qquad (6\text{-}5).$$

The expression of $|\mathbf{A}|^2$ in a reference frame moving with the relativistic velocity u_R, is obtained by the Lorentz transform:

$$z = \gamma_R(\xi+u_R\tau), \qquad \tau = \gamma_R\left(\frac{u_R}{c^2}\xi+\tau\right) \qquad (6\text{-}6).$$

Substituting in (6-5), it turns out that $|\mathbf{A}|^2$ has no τ dependance provided

$$u_R = \frac{\omega_1-\omega_2}{k_1\pm k_2} \qquad (6\text{-}7).$$

In all cases, waves 1 and 2 propagate in opposite directions in the moving frame, with the same frequency and wavenumber (for the free electron laser, ω_2=0, the moving frame is known as the Bambini-Renieri reference frame [9]). In the following we keep only the lower sign in (6-7).

The space and time dependences of the vector potential are contained in the third term of the right hand side of (6-5). Substituting this term in the first equation (6-3) yields an equation of motion for a relativistic electron gas in the laboratory frame. The force resulting from A oscillates at the (low) beat frequency $\omega_1 - \omega_2$. It is called the **ponderomotive force**. The subsequent oscillatory motion of the electrons is resonantly excited when the beat frequency is equal to the plasma frequency. This oscillation induces a longitudinal electric field which has to be included in the equations. It is more convenient to go to the frame

moving with the velocity u_R in which the electron motion is weakly relativistic and use the electric field or the density perturbation as the relevant variable.

In the laboratory frame the longitudinal electric field E fulfills the propagation equation

$$\frac{\partial^2 E}{\partial t^2} - c^2 \nabla^2 E = -\frac{1}{\varepsilon_0}\frac{\partial j}{\partial t} = \frac{e n_0}{\varepsilon_0}\frac{\partial v}{\partial t} \qquad (6\text{-}8)\,.$$

Performing the Lorentz transform, making use of the Poisson equation and neglecting terms in v/c^2, one gets from (6-8), the following equations in the moving frame for the longitudinal E-field and the density perturbation (in the non relativistic limit):

$$\frac{d^2 E}{d\xi^2} + k'^2_D E = -2\frac{e n'_0}{\varepsilon_0}\left(\frac{e}{\gamma_R m_0 c}\right)^2 k'_D A_1 A_2 \cos\left(k'_D \xi\right) = -2\frac{e n'_0}{\varepsilon_0}\frac{k'_D}{\gamma_R^2}\Lambda\cos\left(k'_D \xi\right) \quad (6\text{-}9)\,,$$

$$\frac{d^2 n'}{d\xi^2} + k'^2_D n' = 2 n'_0\left(\frac{e}{\gamma_R m_0 c}\right)^2 k'^2_D A_1 A_2 \sin\left(k'_D \xi\right) = 2 n'_0 \frac{k'^2_D}{\gamma_R^2}\Lambda \sin\left(k'_D \xi\right) \qquad (6\text{-}10)\,.$$

In these equations, $k'_D = (k_1 - k_2)/\gamma_R$ and

$$\Lambda = \left(\frac{e}{m_0 c}\right)^2 A_1 A_2 \qquad (6\text{-}11)$$

is **the interaction parameter**. Since the general form of A is E/ω, the interaction parameter exhibits the usual $I\lambda^2$ dependance.

Equations (6-9) & (6-10) describe the behaviour of an electron plasma wave driven by an external force. This problem can be dealt with assuming that all involved oscillations have a slowly varying amplitude and phase. Accounting for the variations of A_1 and A_2, a set of coupled first order differential equations is then derived. Alternatively, (6-9) represents a typical case of forced oscillations.

It is usually used when the forcing amplitude is nearly constant.

8. Stokes and antistokes forward Raman scattering.

Resonant coupling between two electromagnetic waves and an electron plasma wave is an important nonlinear effect in laser plasma interaction. Whenever one of the E.M. modes has a large initial intensity (as in a laser beam), whilst the other and the plasma oscillation are very weak, this is known as **Stimulated Raman Scattering**. We will restrict ourselves to the case of all waves propagating in the same direction in the laboratory frame (forward scattering). In this frame, the vector potentials obey the usual propagation equation in Lorentz gauge which reads for e.g. the complex potential A_1

$$\frac{\partial^2 A_1}{\partial t^2} - c^2\frac{\partial^2 A_1}{\partial z^2} = \frac{j_1}{\varepsilon_0} \qquad (7\text{-}1)$$

where the current density j_1 in lowest order is

$$j_1 = -\frac{e^2 n_0}{m_0} A_1 - i\frac{e^2}{m_0} n A_2 \qquad (7\text{-}2)\,.$$

The first term in the right hand side is the polarisation current due to A_1; the second term comes from the resonant coupling of A_2 to the plasma wave. Setting

$$A_1 = A_1(z,t)e^{i(k_1 z - \omega_1 t)}\,,\ A_2 = A_2(z,t)e^{i(k_2 z - \omega_2 t)}\,,\ n = n(z,t)e^{i(k_D z - \omega_p t)} \qquad (7\text{-}3)$$

neglecting the second derivatives of the slowly varying amplitude $A_1(z,t)$, and denoting by v_1 the group velocity, one gets a first order partial differential equation

$$2\omega_1\left(\frac{\partial A_1}{\partial t} + v_1\frac{\partial A_1}{\partial z}\right) = -\frac{e^2}{\varepsilon_0 m_0} n A_2 \qquad (7-4).$$

This implies the selection rules: $k_D=k_1-k_2$ and $\omega_p=\omega_1-\omega_2$. By the same token,

$$2\omega_2\left(\frac{\partial A_2}{\partial t} + v_2\frac{\partial A_2}{\partial z}\right) = -\frac{e^2}{\varepsilon_0 m_0} n^* A_1 \qquad (7-5).$$

The second order equation (6-9) is also reduced to first order and given a form analogous to (7-4). Equations are then readily transformed for quantities in the moving frame. The final system is thus:

$$\begin{aligned}
(v_1 - u_R)\frac{dA_1}{d\xi} &= -\frac{e^2}{2\varepsilon_0 m_0 \omega'_1} n' A_2 \\
(v_2 - u_R)\frac{dA_2}{d\xi} &= -\frac{e^2}{2\varepsilon_0 m_0 \omega'_2} n'^* A_1 \qquad (7-6).\\
\frac{dn'}{d\xi} &= n'_0\left(\frac{e}{\gamma_R^{1/2} m_0 c}\right)^2 k'_D A_1 A_2^*
\end{aligned}$$

Such equations were thoroughly investigated in various situations. In all cases, the amplitudes obey the Manley Rowe relations which are best expressed quantum mechanically as

$$1 \text{ photon } \omega_1 \leftrightarrow 1 \text{ photon } \omega_2 + 1 \text{ plasmon } \omega_p .$$

Let first A_1 be a large fixed potential (pump). Initially small A_2 and n' are then to increase exponentially. This is an example of a convective instability with growth rate

$$\Gamma_c = \left(\frac{\omega_p}{\gamma_R^{1/2}}\frac{e}{m_0 c^2}\right) A_1 \qquad (7-7).$$

Actually, waves are damped. The longitudinal plasma waves (e.g.) can be damped either collisionally or via the Landau mechanism. Such effects should

be accounted for in the equations. Then it is found that the growth of the instability occurs if and only if the pump intensity exceeds a threshold which depends upon the damping coefficients of the daughter waves. Many studies were devoted to this problem in the seventies. They were motivated by laser driven inertial confinement fusion. Threshold values were evaluated in both homogeneous and inhomogeneous plasmas. The main result can be summarized as follows: at threshold the product of the pump intensity (in Wcm^{-2}) by the wavelength (in μm) squared is a few $10^{13}\ W\mu^2cm^{-2}$.

Several situations are of interest when A_1 is variable. Assume first that $A_1(0)$ is still a high intensity pump with zero $A_2(0)$ and a small $n'(0)$. The solution of (7-6) is then expressed in terms of Jacobian elliptic functions [10]. The corresponding time history is displayed on figure 7-1a. It exhibits a nonlinear period which depends on $n'(0)$. Since at the begining, a good approximation to the solution is an exponential growth, the physical process is known as **Stokes Raman scattering** by analogy with the behaviour of the solution of the Airy equation. The saturation of the plasma wave is due to pump depletion. When on the contrary, $A_1(0)$ is zero, A_2 is large and $n'(0)$ is still small, the regime is sinusoidal with comparatively low amplitude variations (figure 7-1b). In this case a photon ω_2 combines with a plasmon ω_p to form a photon ω_1: antiStokes Raman scattering.

We now consider the case with initial large amplitudes for both A_1 and A_2. This situation was investigated first by Montgomery [1] who set up equations similar to (7-6), and later in more details by Rosenbluth and Liu [2] who took up the forced oscillator approach. Assume that both laser frequencies are much

greater than the plasma frequency (**beat wave** in an underdense plasma). Then, it is readily shown that **the phase velocity u_R of the plasma wave is equal to the group velocity of the laser waves.**

In order to study the beat wave dynamics, (7-6) is solved first. The result is shown on figure 7-2. Since both $A_1(0)$ and $A_2(0)$ are large, the initial growth of the plasma wave amplitude is fairly linear and much faster than the growth of the Raman scatering near threshold.

8. The Raman cascade.

A single laser wave is able to undergoes forward Raman scattering whenever its intensity is greater than a threshold which depends upon damping mechanisms. The effect goes both ways: either a photon gives rise to a plasmon and a photon with a lower frequency (scattering on the Stokes side) or the photon recombines with a plasmon to produce a photon with a higher frequency (scattering on the antistokes side). The generated wave can grow up to intensities over the threshold value so that it also takes part in a further Raman process.

Consequently, satellite waves with frequency shifts multiple of ω_p can appear on both sides of a given high intensity laser line (figure 8-1): this Raman cascade can lead to turbulence and plasma heating [11].

By the same token, each of the two laser waves participating in the beat wave may be scattered either side. It was considered as a possible saturation mechanism. This cascade can be described by a system of coupled first order differential equations dealing with the complex amplitudes of the modes involved.

The relevant equations were set up by Karttunen and Salomaa [12]. Here the similarity variable ξ is of a temporal nature and the equations read for each E.M. mode labelled j:

$$\frac{dA_j}{d\xi} = \frac{\omega_1}{\omega_j}\left(-A_{j-1}A_p + A_{j+1}A_p^*\right) \qquad (8-1)$$

where ω_1 correspond to the impinging laser wave with the higher frequency and A_p is the amplitude of the plasma mode which in turn satisfies the equation

$$\frac{dA_p}{d\xi} + \left[f(\xi) - 1 + \alpha|A_p|^2\right]A_p = \sum A_j A_{j-1}^* \qquad (8-2)\,.$$

In the left hand side of (9-2) are added terms dealing with the relativistic detuning $\alpha|A_p|^2A_p$ and its compensation by a time varying density $[f(\xi)-1]\,A_p$. A single term only is present in the right hand side of the equations dealing with the modes at both ends of the cascade. These equations are solved numerically for a finite number of modes, usually 30.

Significant results are shown on figure 8-2. Energy cascading towards the lower frequencies improves the quantum efficiency of the beat wave. However, the phase shifts by π every time one of the E.M. waves goes to zero. The conservation of coherence is then questionable. Introducing the relativistic detuning with a large coefficient changes drastically the dynamics. A nonlinear period shows up. The detuning dominates the process. A linear compensation enhances the saturation level of the generated longitudinal plasma wave whilst the electromagnetic spectrum spreads over all allowed modes. This is accompanied by a locking of the relative phase between the two pump waves and the plasma wave. In case of an overcompensation, the relative phase increases indefinitely, the spreading of the spectrum is limited and the plasma wave

saturates at a lower level: a kind of steady state takes place.

9. Connection with the Free Electron Laser.

Consider the dispersion relation for the system made of a cold background plasma with plasma frequency ω_p and a relativistic electron beam with plasma frequency ω_{pb}, and velocity u_b. Denoting by $\varepsilon(k,\omega)$ the high frequency dielectric constant,

$$\varepsilon(k,\omega) = 1 - \frac{\omega_p^2}{\omega^2} - \frac{\omega_{pb}^2}{\gamma_b^2(ku_b-\omega)^2} = 0 \qquad \text{with} \qquad \gamma_b^2 = \frac{1}{1-\frac{u_b^2}{c^2}} \qquad (9\text{-}1)\,.$$

In the Free Electron Laser, there is no background plasma and the dispersion relation reduces to

$$\varepsilon(k,\omega) = 1 - \frac{\omega_{pb}^2}{\gamma_b^2(ku_b-\omega)^2} = 0 \qquad \text{or} \qquad \omega = ku_b \pm \frac{\omega_{pb}}{\gamma_b} \qquad (9\text{-}2)\,.$$

$\gamma_b(ku_b - \omega)$ is the Doppler shifted frequency of the electron wave ω. In the Brillouin diagram (ω,k) the dispersion relation (9-2) is represented by two parallel lines with slope u_b. The upper branch has a positive energy ($\partial\varepsilon/\partial\omega>0$ at $\varepsilon=0$) whereas the lower one has a negative energy ($\partial\varepsilon/\partial\omega<0$ at $\varepsilon=0$)[13]. Now, one may look at the possible couplings of these plasma modes in the beam, to an electromagnetic wave (the laser) and a zero frequency oscillation (the undulator). In figure 9-1, the relevant (ω,k) diagrams are shown for both the laboratory frame and the reference frame in which the beam is at rest: moving frame.

interaction deals with individual electrons rather than with a collective oscillation. Such an effect should happen over a length smaller than the Debye length. On the contrary, collective effects act on a scalelength larger than λ_{De}. In terms of wavenumbers and as an order of magnitude:

$|k| >> |k_{De}|$ holds for individual (Compton) interactions,

$|k| << |k_{De}|$ for collective (Raman) ones.

In a beam in which electrons are shaken by waves, the resulting energy spread $\Delta\gamma_e$ can be used to define the thermal velocity $\langle v_e\rangle$ and the subsequent Debye wavenumber

$$\langle v_e\rangle = c\Delta\gamma_e/\gamma_e \qquad |k_{De}| \approx \omega_p/\langle v_e\rangle \qquad (9\text{-}3)$$

in which γ_e is the Lorentz factor of individual electrons. Now, in a reference frame moving with the phase velocity of the plasma wave, the incident and backscattered electromagnetic modes have the same frequency

$$\omega'_1 = ck'_D/2 \qquad (9\text{-}4).$$

After a Lorentz transformation, one has in the laboratory frame

$$\omega_1 = (1+\beta_e)\gamma_e\omega'_1 \approx 2\gamma_e\omega'_1 = c\gamma_e k'_D, \qquad \text{hence } k'_D = \omega_1/c\gamma_e \qquad (9\text{-}5).$$

The condition for a collective behaviour (Raman scattering) thus implies

$$\omega_1 < \omega_c = \frac{\gamma_e^2\omega_p}{\Delta\gamma_e} \qquad (9\text{-}6)\,.$$

It should be noted that, even in the Compton regime, electrons are periodically bunched as a consequence of a free electron laser process. The period is that of the laser-undulator beats, indicating a self organization of the electron beam in

the form of a plasma wave.

A final remark is noteworthy: since the plasma wave and the laser have the same frequency in the laboratory frame, **the quantum efficiency for plasma wave generation is equal to 1.**

10. Laser-wiggler beat waves in a plasma.

The presence of a background plasma does not changes the three wave couplings involved in the F.E.L. In the case of Raman backscattering, the phase velocity of the laser-undulator beats is

$$u_R = \frac{\omega_1}{k_1 + k_2} \qquad (10\text{-}1)$$

and thereference frame moving with this velocity is the Bambini Renieri (B.R.) frame. From (9-1) a relationship between u_R and the beam velocity u_b is derived viz

$$u_b = u_R \pm \frac{\omega_{pb}}{\gamma_b k_D \sqrt{1 - \frac{\omega_p^2}{\omega_1^2}}} \qquad (10\text{-}2)\,.$$

The upper and lower sign refer to the Cerenkov and inverse Cerenkov regimes respectively. In both cases the Lorentz factor of the beat is

$$\gamma_R^2 = \frac{1}{1 - \frac{u_R^2}{c^2}} = \frac{(k_1+k_2)^2}{(2k_1+k_2)k_2 - \frac{\omega_p^2}{c^2}} \qquad (10\text{-}3)$$

which, since

$$\omega_1^2 = \omega_p^2 + k_1^2 c^2 \qquad (10\text{-}4)$$

implies a divergence for

$$\omega_p^2 - 2c\omega_1 k_2 + k_2^2 c^2 = 0 \qquad (10\text{-}5)\,.$$

In other words, there exists a critical density for the background plasma or a cut-off value for the laser frequency, with the double inequality:

$$n_0 \le n_{0c} = \frac{\varepsilon_0 m_0 (2\omega_1 - ck_2)ck_2}{e^2} \quad \text{or} \quad \omega_1 \ge \omega_{1off} = \frac{\left(\omega_p^2 + k_2^2 c^2\right)}{2ck_2} \qquad (10\text{-}6)\,.$$

The Lorentz factor γ_R depends upon the plasma frequency (i.e. the density) and upon the laser frequency ω_1 as depicted on figure 10-1.

The longitudinal electric field E obeys

$$\frac{\partial^2 E}{\partial t^2} = -\frac{1}{\varepsilon_0}\frac{\partial j}{\partial t} \qquad (10\text{-}7)$$

in which the longitudinal current j has to be calculated after the density perturbations and velocities both in the background plasma and in the beam. Linearized fluid dynamical equations are used for the velocity and the electron density perturbations in the background plasma and in the beam as well. The result is a second order partial differential equation for the electric field in the B.R. reference frame (no time dependance, non relativistic motion):

$$\frac{d^2 E}{d\xi^2} = -k'^2_D E + 2\frac{m_0 c\omega_1}{e}\Lambda\left[\left(\frac{\omega_p}{\omega_1}\right)^2 + \frac{1}{\gamma_R}\right]\cos\left(k'_D \xi\right) \qquad (10\text{-}8)\,.$$

Now, in the interaction parameter Λ, for the undulator (magnetic field B_2): $A_2 = B_2/k_2$. In the right hand side of (10-8), the first term in the [ ] bracket is the non resonant contribution of the background plasma and the second one is the resonant contribution of the beam.

Assume A_1, A_2 and E have slowly variable amplitudes: these are found to obey a first order system of 3 coupled differential equations. The undulator is equivalent to a very high intensity electromagnetic wave. Λ is made large with a

comparatively moderate laser intensity. Since the quantum efficiency is unity, the plasma wave amplitude is obviously bounded by the laser amplitude.

The saturation results from the usual contributions of many mechanisms: pump depletion, cascading, collisions, relativistic effects... Since the static magnetic field of the undulator is set up over a limited number of periods, the finite size might also influence the growth of the plasma wave. This can be accounted for by introducing a phenomenological damping term in the left hand side of equation (10-8) in which the reciprocal of the undulator length L' (measured in the moving frame) appears as an effective collision frequency. This approximation was proved to work for parametric instabilities in bounded plasmas [15]. Now, the second order equation for E is:

$$\frac{d^2E}{d\xi^2} + \frac{1}{L'}\frac{dE}{d\xi} = -\left(1 - \alpha|E|^2\right)k'^2_D E + 2\frac{m_0 c\omega_1}{e}\Lambda\left[\left(\frac{\omega_p}{\omega_1}\right)^2 + \frac{1}{\gamma_R}\right]\cos\left(k'_D\xi\right) \qquad (10\text{-}9)\,.$$

With constant Λ, (10-9) is a Duffing's equation. The effective damping and the relativistic detuning can also be included in the first order system which accounts for pump depletion.

When the effective damping and pump depletion are small, the plasma wave amplitude is limited by the relativistic detuning. A maximum electric field is calculated after the Duffing's equation in the case of growth from a very low level

$$E_{Max} = \frac{cm_0\omega_1}{e}\left[\left(\frac{\omega_p}{\omega_1}\right)^2 + \frac{1}{\gamma_R}\right]\left(\frac{16\,\Lambda}{3}\right)^{1/3} \qquad (10\text{-}10)\,.$$

The accelerating field is the smaller of two: the electric field given in (10-10) and the laser electric field. Furthermore, it has to be larger than the driving longitudinal field, otherwise there would be no plasma and the system would operate in the so called Inverse Free Electron Laser (I.F.E.L.) regime. Then, (10-10) holds provided

$$\frac{cm_0\omega_1}{e}\frac{\Lambda}{\gamma_R} < \frac{cm_0\omega_1}{e}\left[\left(\frac{\omega_p}{\omega_1}\right)^2 + \frac{1}{\gamma_R}\right]\left(\frac{16\,\Lambda}{3}\right)^{1/3} < E_1 = \frac{cm_0\omega_1}{e}\frac{cm_0\Lambda}{eA_2} \qquad (10\text{-}11)$$

which implies

$$\gamma_R > \gamma_{Rcrit} = \frac{eA_2}{m_0c} = \frac{eB_2}{m_0ck_2} \qquad (10\text{-}12)\,.$$

When the Lorentz factor of the B.R. frame surpasses the critical value, one has the situation depicted in figure 10-2 which shows plasma enhancement of the longitudinal field induced by laser-wiggler beating when the interaction parameter Λ is smaller than about 0.6.

In this process, since its frequency is much larger than the background plasma frequency, the generated plasma wave has a nonzero group velocity. It can be launched through a plasma longer than the undulator. The extra length could be used as an accelerating section separated from the region where the plasma wave is created.

11. Evaluation of saturation mechanisms.

Besides pump depletion, the actual amplitude of the longitudinal field is expected to saturate thanks to a large number of various possible processes: wavebreaking, relativistic oscillatory motion of the electrons in the wave, competing instabilities, cascading, collisional or Landau damping... Examples of growth and saturation of the electron plasma wave were given in the case of the Raman cascade. In particular the role of a compensating detuning $f(\xi)$ was investigated.

The term $f(\xi)$ may be included in the equations for other reasons, for instance

the onset of a modulational instability which results from the coupling of a high amplitude plasma wave and ion-acoustic oscillations. The latter induce a sinusoidal detuning with a period much longer than the electron wave period and growth rate. Choose the longitudinal electric field E as the significant variable. In the left hand side of the forced oscillator equation (6-9), one may add a cubic term $\alpha |E|^2 E$ accounting for relativistic electron oscillations and a periodic $f(\xi)$ representing the modulational instability. One then gets a modified Duffing's equation

$$\frac{d^2E}{d\xi^2} + \Gamma\frac{dE}{d\xi} + \left[f(\xi) - \alpha|E|^2\right]E = -F\cos\xi \qquad (11\text{-}1)$$

in which Γ is a damping coefficient (collisionnal or Landau) and the driving amplitude F is proportionnal to the interaction parameter Λ. This equation can be used to investigate qualitative features. A computationnal result is shown on figure 11-1. The electron wave saturates at a level which remains about constant for a while and finally decreases exponentially.

A comparative review of beatwave saturation mechanisms was given by P. Mora [16] for typical conditions of laser irradiation. The mechanisms considered are:

- relativistic detuning,
- linear detuning i.e. approximate frequency adjustment,
- lateral plasma expansion due to transverse ponderomotive potential associated either with the focused laser beam or the generated electron plasma wave itself,
- the modulational instability as investigated in [17],
- collisions.

For any one of these, the maximum relative amplitude $\Delta n/n$ of the density perturbation in the plasma wave scales as $I\lambda^2$ where I and λ are respectively the laser wavelength and intensity. The results are best presented diagrammatically. Figure 11-2 (after [16]) refers to the following plasma parameters: electron density 10^{17} cm^{-3}, temperature 40e.V., focal spot diameter 100μm. They show that in the range of $I\lambda^2$ expected for particle acceleration the main limiting processes are the linear detuning (5% error with respect to the density for resonance) and the modulational instability.

12. Longitudinal wave generation vs. plasma heating.

When a high intensity laser beam impinges onto a plasma, part of the energy is absorbed thanks to inverse bremsstrahlung, a mechanism which depends on electron ion-collissions. These collisions also act as a damping process for the longitudinal plasma wave. They are density and temperature dependant.

Taking up the usual formulas for Coulomb collisions, the damping term in the modified Duffing equation of the type (11-1) is proportional to $T_e^{-3/2}$. Now, the electron temperature T_e is given by a rate equation the right hand side of which is the balance between gains due to laser energy absorption by inverse bremmstrahlung and any kind of heat losses which can be simply modeled by a constant coefficient times T_e/ξ. Altogether, the longitudinal wave electric field and the electron temperature are given by the solutions of coupled equations of the form

$$\frac{d^2E}{d\xi^2} + \frac{\Gamma}{T_e^{3/2}}\frac{dE}{d\xi} + \left[f(\xi) - \alpha|E|^2\right]E = -F\,I(\xi)\cos\xi$$

$$\frac{dT_e}{d\xi} = \frac{G}{T_e^{3/2}}I(\xi) - P\frac{T_e}{\xi} \qquad (12\text{-}1)\,.$$

Typical results are shown on figures 12-1 and 12-2. The laser pulse is gaussian. It turns out that the shape of $E(\xi)$ depends on the ratio Γ/G. for a low value of this parameter, the nonlinear period is clearly visible. On the contrary, damping dominates when Γ/G is large. The maximum value of E is about the same in both cases. In the investigated range of parameters, the growth and saturation of the plasma wave are not dramatically changed by the occurence of laser heating of the plamsa.

13. Laser induced wakefield.

It has been known for quite a long time that a relativistic bunch of charged particles passing through a plasma perturb the electron gas. A wake is induced, i.e. a longitudinal plasma wave follows the bunch. The same effect is to arise with any concentration of electromagnetic energy propagating with the speed of light e.g. very short intense laser pulses. The perturbation of the electron gas is then due to the pondromotive force associated with the rapidly varying amplitude of the electric field in the pulse. Following Gorbunov and Kirsanov [4], the coupled equations for the transverse electron velocity $v_\perp$ and the longitudinal density perturbation n are

$$c^2\frac{\partial^2 v_\perp}{\partial z^2} - \frac{\partial^2 v_\perp}{\partial t^2} - \omega_p^2 v_\perp = -\frac{1}{2}\frac{\partial^2 v_\perp^3}{\partial z^2} + \frac{1}{2c^2}\frac{\partial^2 v_\perp^3}{\partial t^2} + \frac{\omega_p^2}{n_0}nv_\perp \qquad (13\text{-}1)$$

$$\frac{\partial^2 n}{\partial t^2} + \omega_p^2 n = \frac{n_0}{2}\frac{\partial^2 v_\perp^2}{\partial z^2} \qquad (13\text{-}2)\,.$$

The longitudinal electrostatic potential is given by Poisson's equation

$$\frac{\partial^2 \Phi}{\partial z^2} = -\frac{en}{\varepsilon_0} \qquad (13\text{-}3)\,.$$

For a transverse velocity of the form

$$v_\perp(z,t) = \frac{e}{2m_0\omega}\left[E(\xi)e^{i(kz-\omega t)} + C.C.\right] \qquad (13\text{-}4)\,.$$

where the amplitude $E(\xi)$ of the laser electric field is a slowly varying function of the similarity variable $\xi=z-v_g t$, v_g being the group velocity, and provided the pulse length is shorter than the plasma wavelength

$$\Phi(\xi) = \Phi_0\sin(k_p\xi+\psi) \qquad \text{with} \qquad \Phi_0 = \frac{k_p e}{4m_0}\int_{-\infty}^{\infty}|E(\xi)|^2 d\xi \qquad (13\text{-}5)$$

in which $k_p=\omega/v_g\approx\omega/c$. The longitudinal electric field is:

$$E = \frac{ek_p^2}{\varepsilon_0 m_0\omega^2}F \approx \frac{e}{\varepsilon_0 m_0 c^2}\frac{\omega_p^2}{\omega^2}F \qquad \text{where} \qquad F = \int_{-\infty}^{\infty}\varepsilon_0|E|^2 d\xi \qquad (13\text{-}6)$$

is a fluence i.e. the energy which has passed through a unit surface. F is also the product $I\Delta t$ of the laser intensity by the pulse duration. Putting numbers in the formula yields:

$$E(Vm^{-1}) = 2.2\,10^9\frac{\omega_p^2}{\omega^2}I(Wcm^{-2})\Delta t \qquad (13\text{-}7)\,.$$

If for instance, the electron plasma density is 10^{17} cm^{-3}, the wavelength of the longitudinal oscillation is 100 μm. Taking $\Delta t = 3\,10^{-13}$ s., the intensity required to

obtain 10^9 Vm^{-1} is $1.5\ 10^{14}$ Wcm^{-2} from a CO_2 laser ($\omega_p/\omega=10^{-1}$) and $1.5\ 10^{16}$ Wcm^{-2} from a Nd laser ($\omega_p/\omega=10^{-2}$).

These values are of the same order of magnitude as those necessary for beatwave generation. Strong focusing of the laser beam is requested. The length (twice the Rayleigh length) available for plasma wave generation is limited to a few millimeters unless self focusing takes place. There is still a definite advantage of the laser induced wakefield. No resonance condition is to be satisfied.

14. Requirements for lasers.

Lasers might be used for plasma creation, beatwave generation or wakefield generation. For all these potential uses, the requirements are very much alike. If one has in mind the application to particle accelerators, further constraints have to be accounted for. Indeed, besides the energy, the devices should provide a sufficient number of expected events thanks to a **high luminosity**. This parameter is proportional to the **repetition rate**: a convenient value the lasers should mandatorily match is **1 kHz**.

A high energy particle accelerator is obviously expensive. Routine operation is also costly. It is important that the machine be as efficient as possible. To this end, the **overall laser efficiency has to be over 10%**.

The beat wave mechanisms leads to requirements on wavelength, power, and pulse duration. It has been shown:

i) that the electric field E_D in the plasma wave which determines the acceleration gradient increases as the square root of the plasma density;

ii) that the Lorentz factor γ_R associated with the phase velocity is proportional to ω_0/ω_p. One wants high values for both E_D and γ_R which imply a dense plasma and consequently a **small laser wavelength**.

High laser powers are also needed. First, in beat wave generation the saturation amplitude, and hence the acceleration energy W_A, turns out to scale as $(I\lambda^2)^{1/3}$. This constraint is somewhat relaxed in the "surfatron" [18] and laser wiggler beat wave schemes. However, consider on table 2 the calculated values of

acceleration energies and lengths in beatwave generation with saturation by relativistic detuning. It appears difficult to match the focal volume of an optical system to the acceleration length. Now, light self-focusing was evidenced in numerical simulations [19]. The mechanism which comes from either ponderomotive or relativistic effects, provides a high intensity over long distances. In both cases the laser power (not the intensity !) has to exceed a wavelength dependent threshold.

Finally, one has to look at the pulse duration. In beatwave generation, it should not be larger than a few nonlinear periods. In practice, this condition leads to **1-50 ns pulses**. In plasma creation by multiphotonic ionization, and in plasma wakefield, 1 p.s is an upper boudary.

The above requirements: high repetition rates over long periods of time (days or months), 10 % efficiency, short wavelength, high power and picosecond pulses, look rather contradictory. No existing laser meets all of them, as can be seen in Table 3.

The KrF laser exhibits some appealing features. The main issue is how to efficiently extract the pump energy with picosecond pulses, a so far unsolved problem. Angle multiplexing as used in Inertial Fusion is concievable. But, in recombining the beams, one should be very careful about coherence which is essential in driving the plasma wave. Table 4 gives after J.J. Ewing [20] , the main properties of both a KrF and a CO_2 laser designed for a 10 TeV electron accelerator. The latter is well suited for proof-of-principle demonstrations as shown by preliminary experiments in the U.S. (U.C.L.A.) and Canada (I.N.R.S.).

Acceleration of elementary particles in laser plasma interaction has been demonstrated on a very small scale: 1 GeV/m over1mm only. It is considered

seriously by high energy physicists as a very promising way to reach energies beyond a few TeV. However the subject is still in its infancy. The accelerators of the next generation will be designed and built by extrapolating known and reliable techniques. This leaves about 20 years from now:

i) to investigate all the physics relevant to laser-driven acceleration of particles in plasmas;

ii) to design laser sources suited to the job.

If one looks back at the progress in the physics and the technology of high-power lasers designed for Inertial Fusion, one sees an increase in power by 6 orders of magnitudes over the past 20 years. This is indeed a remarkable achievement. There is no doubt that, provided the demand and the motivation exist, a similar evolution will occur: by A.D. 2010, laser properties could be close enough to the requirements of accelerator physics, in time for a future generation of machines.

References

1. D.C. Montgomery, *Physica* **31** (1965) 693.
2. M.N. Rosenbluth and C.S. Liu, *Phys. Rev. Lett.* **29** (1972) 701.
3. T. Tajima & J.M. Dawson, *Phys. Rev. Lett.* **43** (1979) 267.
4. L.M. Gorbunov and V.I. Kirsanov, *Soviet Phys. J.E.T.P.* **66**(1987)290.
5. A.E. Dangor et al. IEEE *Trans. Plasma Sci.* **PS-15**(1987)161.
6. Yu. P. Raizer, *Laser Induced Breakdown of Gases*, 1977.
7. J.P. Bardet et al. to appear in *Laser and Particle Beams*, 1989.
8. D.L. Matthews et al. *J. de Physique, supplément,* **47**(1986)C6-1
   P. Jaeglé et al. *J. de Physique, supplément,* **47**(1986)C6-31
9. A. Bambini and A. Renieri, *Lett. Nuov. Cim.* **21** (1978) 239.
10. R.B. Bingham and C.N. Lashmore-Davies, *Nucl. Fusion* **16**(1976)67.
11. B.I. Cohen, A.N. Kaufman, K.M. Watson, *Phys. Rev. Lett.* **29** (1972) 581.
12. S.J. Karttunen & R.R.E. Salomaa, *Phys. Rev. Lett.* **56** (1986) 604.
13. see e.g. L.D. Landau and E.M. Lifshitz, *Electrodynamique des Milieux Continus* , Mir, Moscou (1969).
14. R. Bonifacio and F. Casagrande, *Optics Comm.* **50** (1984) 251,
    J.B. Murphy and C. Pellegrini, *Nucl. Instrum. Methods* **A257** (1985) 159.
15. R. White et al. *Nuclear Fusion* **14** (1974) 45.
16. P. Mora, *Revue Phys. App.* **23**(1988)1489.
17. P. Mora et al. *Phys. Rev. Lett.* **61**(1988)1611.
18. T. Katsouleas & J.M. Dawson, *Phys. Rev. Lett.* **29**(1983)392.
19. C. Joshi et al. *Nature,* **311**(1984)525.
20. J.J. Ewing, Workshop on Advanced Accelerator Concepts, Madison August 1986, unpublished.

Table 1.

LASER GENERATION OF PLASMAS

		density (ecm^{-3})	comments
Gas breakdown	in quiet gas	10^{15}-10^{17}	multiphoton ionization produces completely ionized plasmas with a very uniform electron density [5]. Efficiency is questionable.
	in gas jets	10^{16}-10^{17}	uniformity is questionable.
Resonant gas breakdown		10^{15}-10^{17}	Efficient, but so far restricted to metal vapour.
Interaction with solid surfaces		10^{16}-10^{20}	adjustable length.
Interaction with thin foils		10^{16}-10^{20}	short but controlable.

Table2

MAXIMUM ENERGIES AND ACCELERATION LENGTHS

Laser wavelength (μm)	10	1	0.25	
Intensity (Wcm-2)	1.3×10^{15}	1.3×10^{17}	2×10^{18}	
Electron density (cm-3)				**Gradient** (GeV/m)
10^{15}	**10 GeV** 4 m	**1 TeV** 400 m	**16 TeV** 6.4 km	**2.5**
10^{16}	**1 GeV** 13 cm	**100 GeV** 1.3 m	**1.6 TeV** 210 m	**6**
10^{17}	**100 MeV** 4 mm	**10 GeV** 40 cm	**160 GeV** 6.4 m	**25**
10^{18}	**10 MeV** 0.13 mm	**1 GeV** 1.3. cm	**16 GeV** 21 cm	**60**
10^{19}		**100 MeV** 0.4 mm	**1.6 GeV** 6.4 mm	**250**

Table 3

STATE-OF-THE-ART LASERS AND ACCELERATOR REQUIREMENTS

LASER	λ(μm)	SMALL λ	PICOSECOND PULSES	ENERGY 10^2-10^4J	REP. RATE 1 KHz	EFFICIENCY ≥10 %
CO2	10	NO	Possible	Proven	Possible	Proven
HF	2	NO	NO	Possible	Possible	Proven
Nd	1	Yes	Proven	Proven	NO	NO
KrF	0.25	Yes	Questionable	Possible	Possible	Possible

Table 4.

DATA FOR A LASER IN A 10 TeV ACCELERATOR

Assume: laser / beat wave conversion efficiency is 25 %

	CO_2	KrF
λ_2-λ_1	1μm	37Å *
Plasma electron density	$10^{17}cm^{-3}$	$4\ 10^{18}cm^{-3}$
γ_R	10	68
l_A	0.6 cm	3.8 cm
Power for self-focusing	0.47 TW	21 TW
Pulse duration	3 psec.	3 psec.**
Energy/pulse	1.4 J.	63 J.
Total length	660 m	104 m

* feasible by Raman shift in H_2

** DREAM !

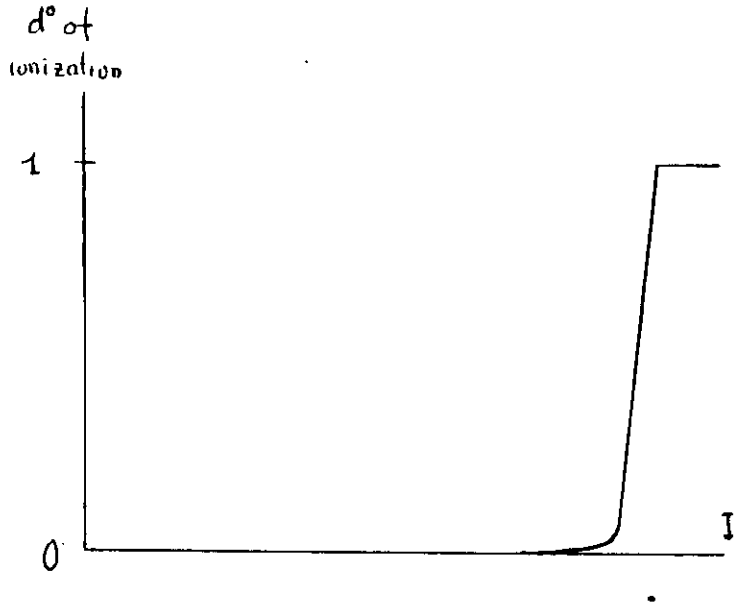

3-1

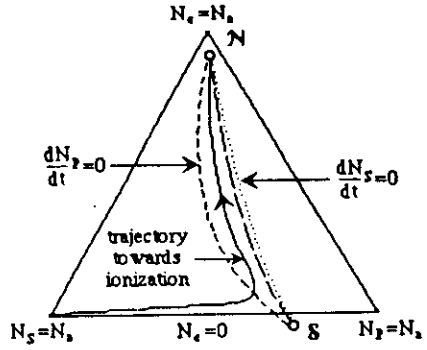

4-1

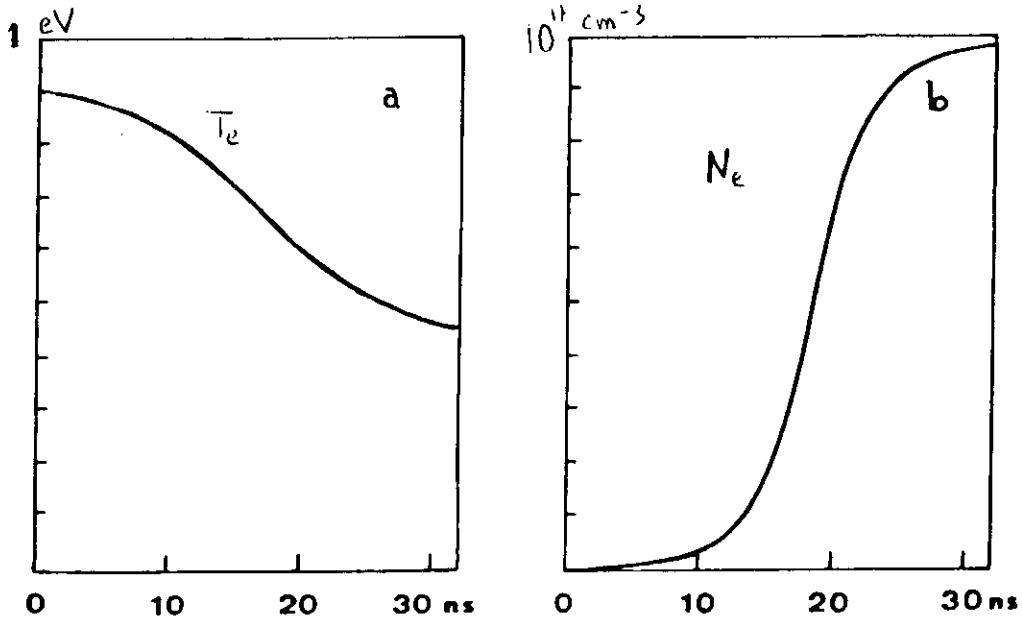

4-2

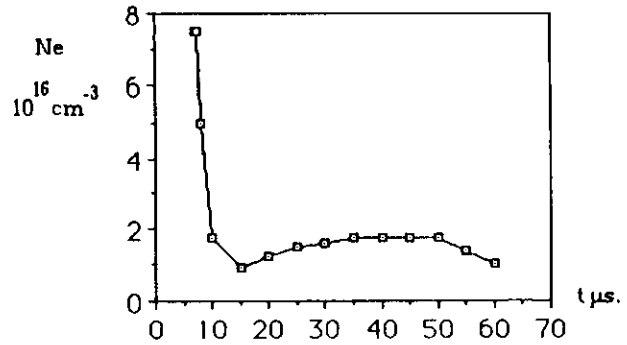

a

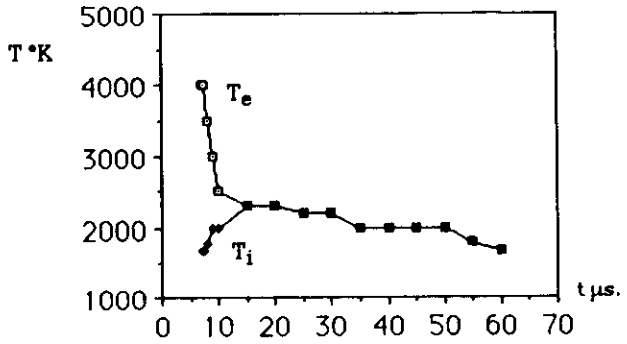

b

Figure 4-3. Time histories from spectroscopic diagnostic a) electron density, b) electron and ion temperatures.

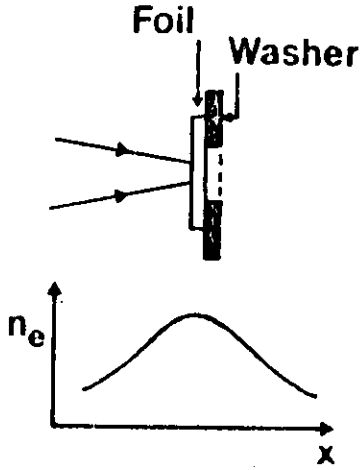

5-1

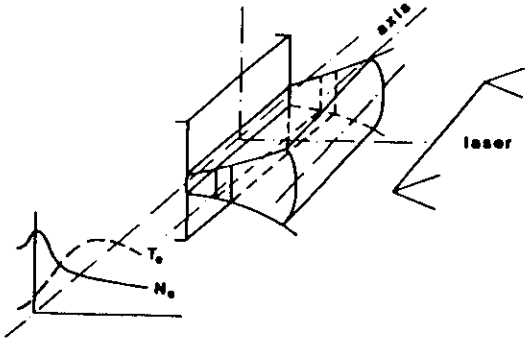

5-2 This sketch presents some of the general features of a plasma column produced by a cylindrical focusing of laser-beam. The behaviour of electron density and temperature, perpendiculary to the target surface, is represented on the left side. If the illumination is constant along the focal line, the plasma is homogeneous in the axial direction which is used for gain measurements.

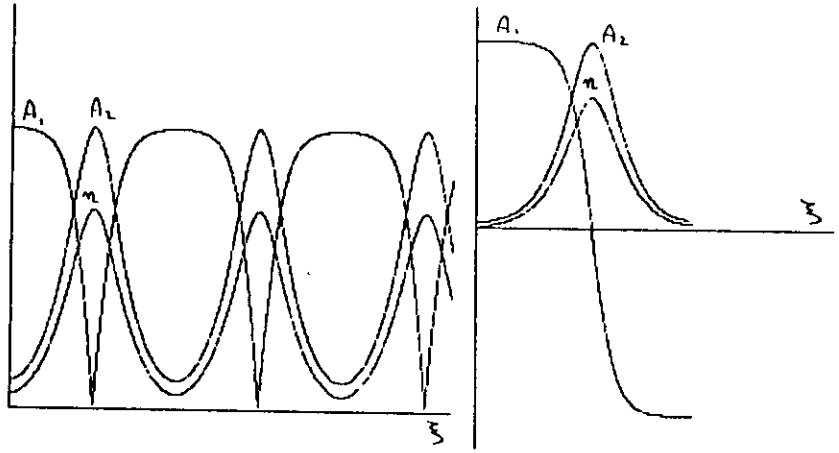

7-1-a Time history of amplitudes in Stokes Raman scattering
a) periodic regime; b) solitons.

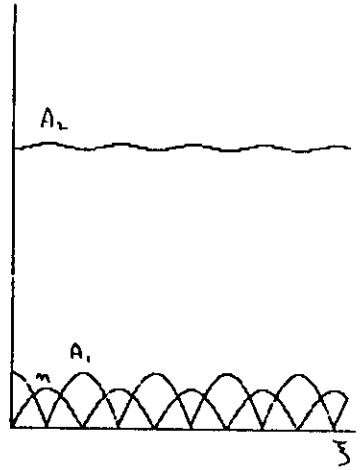

7.1.b AntiStokes Raman scattering

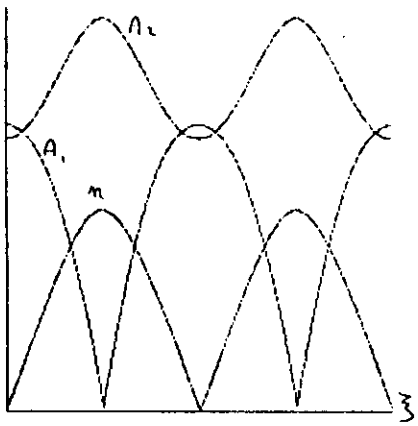

7-2a Beat wave saturation by pump depletion.

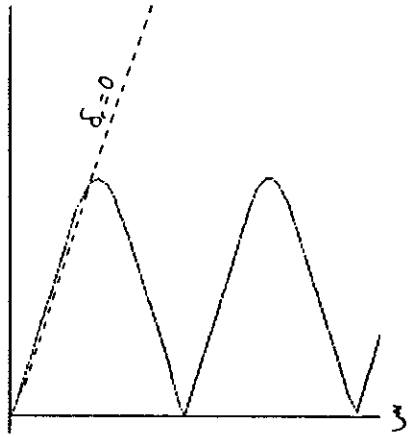

7-2b Beat wave saturation by relativistic detuning.

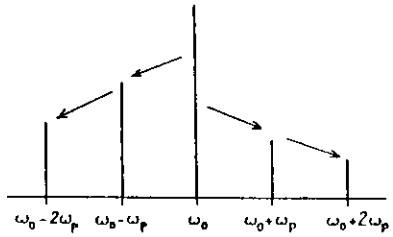

8-1. Radiation spectrum induced by a Raman cascade

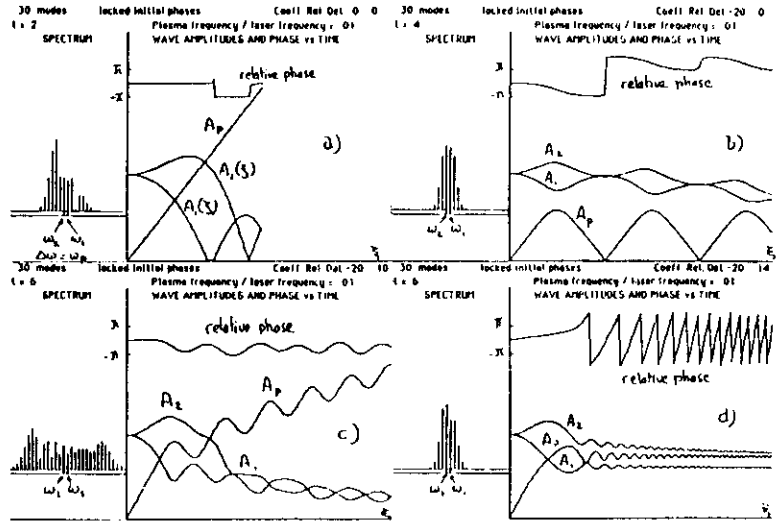

8-2 The Raman cascade. a) without relativistic detuning nor compensation; b) with relativistic detuning, no compensation; c) relativistic detuning, linear compensation, d) overcompensation of the relativistic detuning.

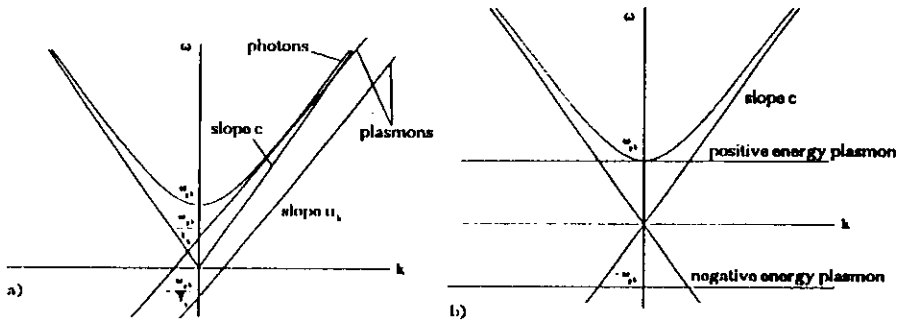

9 - 1.
Dispersion relations for electromagnetic waves and plasma waves in a relativistic beam. a) laboratory frame; b) moving frame.

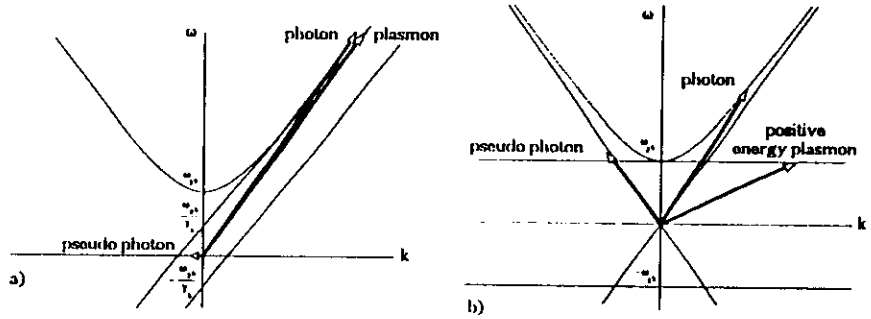

9 - 2.
Raman backscattering in the inverse Cerenkov regime.
a) laboratory frame; b) moving frame.

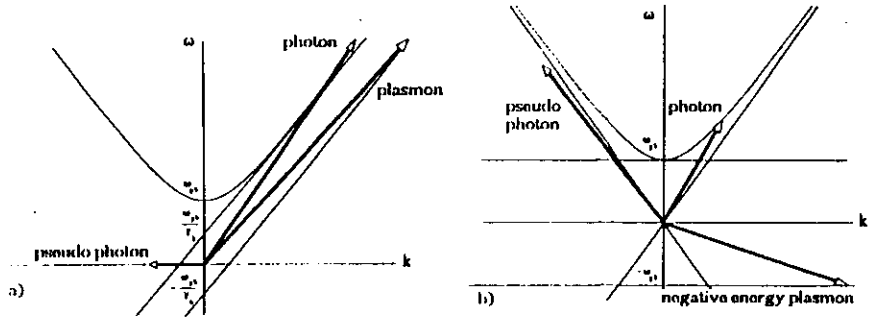

9 - 3.
Raman scattering in the Cerenkov regime.
a) laboratory frame; b) moving frame.

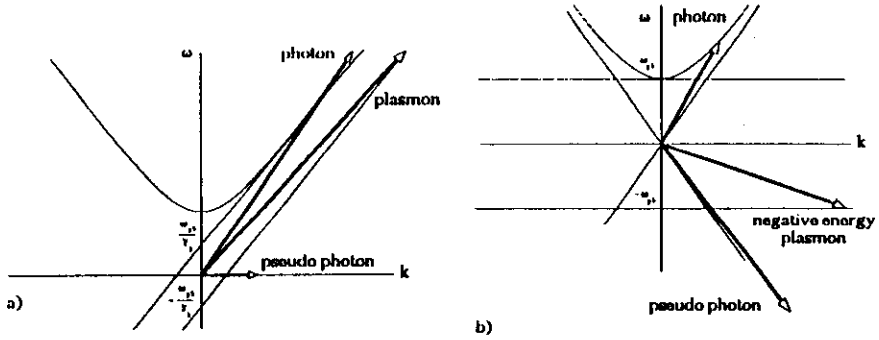

9 - 4.
Explosive instability. a) laboratory frame; b) moving frame.

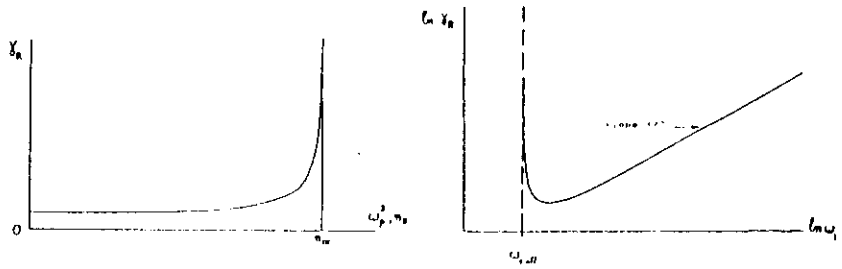

10 - 1 Lorentz factor for the B.R. frame versus:
a) the plasma density; b) the laser frequency.

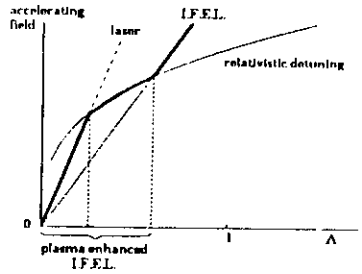

10 - 2 Accelerating field versus interaction parameter.

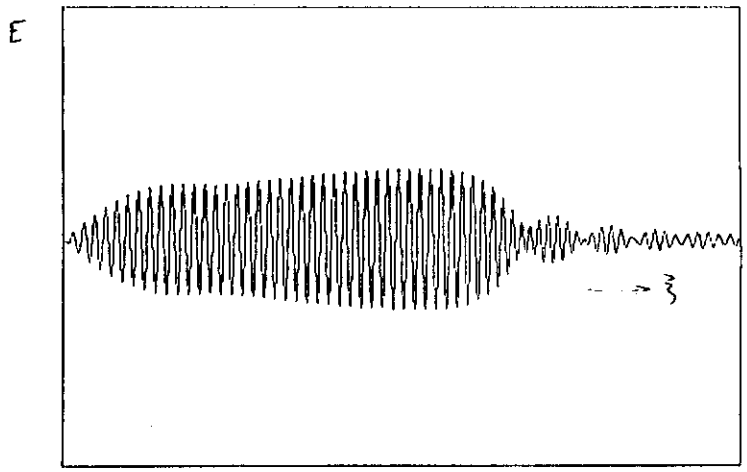

II - 1

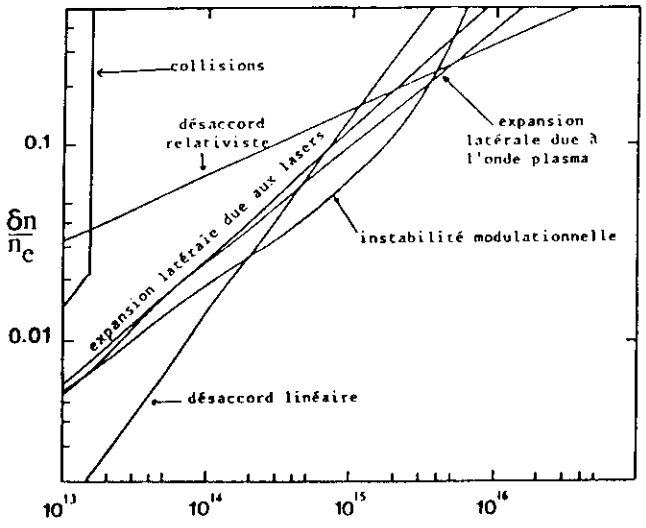

II - 2

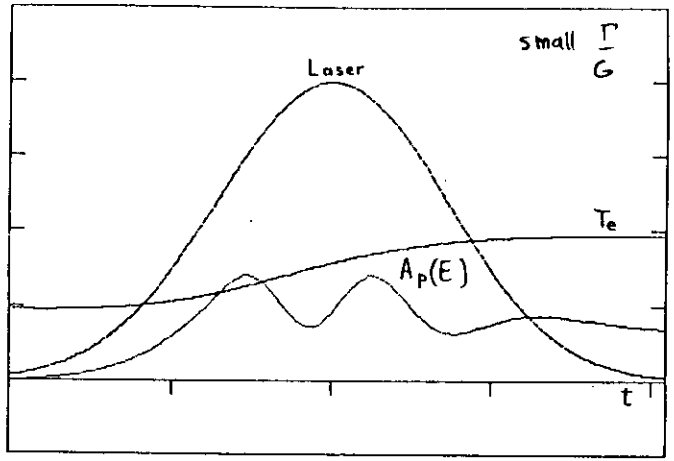

12 - 1

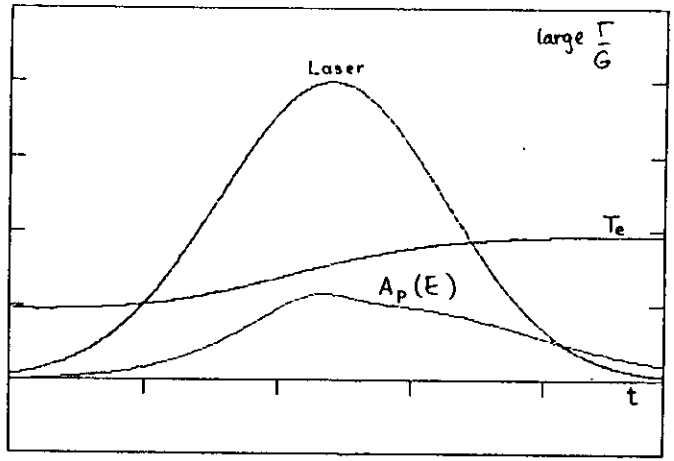

12 - 2